Ionics (2010) 16:33–38
DOI 10.1007/s11581-009-0324-6

ORIGINAL PAPER

Electrodeposition of platinum on tourmaline and application as an electrocatalyst for oxidation of methanol

Jin-Hong Li · Li-Zhen Fan · Li-Bing Liao

Received: 19 November 2008 / Revised: 15 December 2008 / Accepted: 14 January 2009 / Published online: 7 February 2009

Abstract A composite electrode of Pt nanoparticles coupled with tourmaline is prepared on glassy carbon (GC) disk electrode via electrodeposition. The nanocomposite of Pt/tourmaline is characterized by scanning electron microscopy, X-ray photoelectron spectroscopy, X-ray powder diffraction, and transmission electron microscopy examinations linked with energy dispersive X-ray analysis. The electrocatalytic performance of the composite electrode (Pt/tourmaline/GC) is investigated in electrocatalysis oxidation of methanol at room temperature by cyclic voltammetry and chronoamperometry. It is indicated that Pt nanoparticles with size of ~5 nm are uniformly assembled along the tourmaline particles and Pt exists in metallic and oxidated states confirmed by XPS. The results of electro-oxidation of methanol show that Pt/tourmaline catalyst is catalytically more active and stable than platinum-modified GC electrode, and the onset potential of Pt/tourmaline shifts 0.15 V to the negative side, and also the current density is significantly enhanced.

Keywords Composite electrode · Tourmaline · Electrodeposition · Electrocatalyst · Methanol oxidation

J.-H. Li · L.-B. Liao
Beijing Key Laboratory of Water Resource and Engineering,
School of Materials Science and Technology,
China University of Geosciences,
Beijing 100083, China

L.-Z. Fan (✉)
School of Materials Science and Engineering,
University of Science and Technology Beijing,
Beijing 100083, China
e-mail: fanlizhen@mater.ustb.edu.cn

Introduction

Direct methanol fuel cells (DMFCs) have attracted much attention as a clean and effective power source [1, 2]. However, the adsorbed intermediates (e.g., CO) in methanol oxidation reaction cause kinetic impediment, resulting in overpotential of 0.1–0.6 V [3]. The sluggish kinetic rate of methanol oxidation resulting from poor activity and low utilization efficiency of noble metal catalysts pose a challenge to the development of DMFCs [4, 5]. Pure platinum as a catalyst for methanol electro-oxidation is not very effective because Pt is readily poisoned by strongly adsorbed intermediates, i.e., the so-called Pt poison phenomenon [6–8]. A most common way to overcome Pt poison is to select a proper electrode with further modification such as metals that are capable of absorbing oxygenated species (e.g., OH) from the dissociation of water at low potentials [9]. The modified layer is able to oxidize the intermediates completely to CO_2, and generally the modifier should facilitate cleavage of C–C in the alcohols [10]. Presently, conductive boron-doped electrode has emerged as an attractive electrode material due to its wide electrochemical potential window, high chemical and thermal stability, extreme hardness and corrosion resistance, and a very low capacitive background current [11, 12, 13, 14]. Avaca et al. found that the boron-doped diamond electrode possessed high stability at extreme positive and negative potential under both acidic and alkaline conditions, without any evidence of structure degradation in catalyzing the methanol oxidation reaction [15]. Montilla and coworkers prepared a Pt-modified boron-doped diamond electrode by electrochemical method and applied it in catalyzing methanol oxidation [16]. The activity was found to be satisfactory, although there is a loss of 65% of the initial Pt particles after cycling several times.

Tourmaline is a kind of borosilicate mineral belonging to the trigonal space group. The general chemical formula can be written as $NaMg_3Al_6[Si_6O_{18}](BO_3)_3(OH)_4$, where Al^{3+} can be replaced by Fe^{3+}, Na^+ by Li^+, and Mg^{2+} by Fe^{2+} or Li^+–Al^{3+} [17]. One of the most important features of tourmaline is the possession of spontaneous and permanent poles. Due to the strong electric field and high irradiation of far infrared around its surface, tourmaline has been widely used in many fields such as shielding of electromagnetic wave [18], releasing of negative ions, and as ecomaterials in environment purification [17, 19], pressure sensor [20], infrared sensor [21], etc. In view of the properties of tourmaline such as permanent or spontaneous polarity and high radiancy of far infrared that favors producing negative ions [22], herein, we proposed a new tourmaline-based Pt nanocatalyst (Pt/tourmaline) via method of electrodeposition and employ it on glassy carbon electrode (GC) in electrocatalyzing oxidation of methanol. The results showed that the prepared Pt/tourmaline-modified GC (Pt/tourmaline/GC) is relatively highly active with prominent stability in room temperature for electro-oxidation of methanol. This method provides new insight in developing low-cost and high-performance, tourmaline-based electrodes.

Experimental

Tourmaline was collected from Arertai, Xinjiang Province, China. The chemical components were analyzed by electron probe microanalysis (EPMA-1600, averaged by 30 points) and the phase was identified by XRD analysis. On the principle of mass balance and according to the composition of ideal tourmaline, the chemical formula was evaluated as $(Na_{0.629}Ca_{0.195})(Mg_{2.007}Fe_{0.138})(Al_{5.054})(Si_{4.813}Ti_{0.068})O_{18}(BO_3)_3(F,OH)_4$ calculated by LINPRO software. The tourmaline can be classified into dravite series. Other chemical reagents such as H_2PtCl_6, H_2SO_4, and methanol were purchased from Beijing Chemical Reagent Ltd. High purity water was prepared from distilled water filtered with a Millipore Milli-Q system (MQ water, 18.2 MΩ).

The Pt/tourmaline-modified electrode (Pt/tourmaline/GC) was prepared by electrodeposition of H_2PtCl_6 onto the tourmaline-modified glassy carbon electrode (GC, 3 mm diameter, Bioanalytical Systems Inc.). GC electrode was firstly polished with emery paper and then with aqueous slurries of fine alumina powders (0.3 and 0.05 μm) on a polishing cloth. The electrodes were rinsed with MQ water and acetone in an ultrasonic bath, each for 5 min, and were extensively rinsed with MQ water before use. Then the clean GC electrode was deposited with a drop (0.05 ml) of tourmaline aqueous dispersion (0.1 g/ml) followed by drying under irradiation of infrared lamp. Electrodeposition of Pt nanoparticles on the tourmaline-modified electrode was carried out in KPF_6 (0.1 M) and H_2PtCl_6 (0.1 M) solution at −1.5 V (referred to an Ag/AgCl electrode (KCl saturated)) for 40 min. To evaluate the content of Pt in the modified layer of Pt/tourmaline/GC, we test the parallel sample by XPS technique. The content of Pt is 0.48 mg/cm^2. This sample of modified GC electrode was denoted as Pt/tourmaline/GC. The electrodeposited Pt nanoparticles were rinsed thoroughly with MQ water prior to electrochemical measurements. For comparison, we also conducted a control experiment to prepare Pt-modified GC (Pt/GC) and tourmaline-modified GC electrode (tourmaline/GC). In preparing Pt/GC, H_2PtCl_6 aqueous solution was firstly reduced by $NaBH_4$ to get a dispersion of Pt(0) particles and then a droplet of Pt(0) dispersion was deposited on the GC electrode before it was dried. By controlling the initial Pt concentration, both electrodes including Pt/tourmaline/GC and the Pt-modified GC have the same content of Pt ~0.5 mg/cm^2. Tourmaline/GC electrode was prepared by dropping 0.05 ml tourmaline dispersion (0.1 g/ml) onto the GC electrode. The tourmaline layer was attached to the GC by a droplet (5 μl) of a dilute aqueous Nafion solution.

The X-ray photoelectron spectroscopy (XPS) spectra of the Pt/tourmaline composite were collected on an ESCALab220i-XL spectrometer at a pressure of about 3×10^{-9} mbar using Mg Kα as the excitation source ($h\nu$=1,253.6 eV) and operating at 15 kV and 20 mA. The C1s binding energy was set to 284.8 eV as the energy calibration. The X-ray powder diffraction (XRD) patterns were collected on an X-ray diffractometer (DMAX) operated at 40 kV and 40 mA with nickel-filtered Cu Kα radiation λ=1.5419 Å. Transmission electron microscopy (TEM) equipped with X-ray energy dispersive analysis (EDS) was performed on a transmission electron microscope (Philips, Tecnai F20) at a operating voltage of 200 kV, and the images were electron-

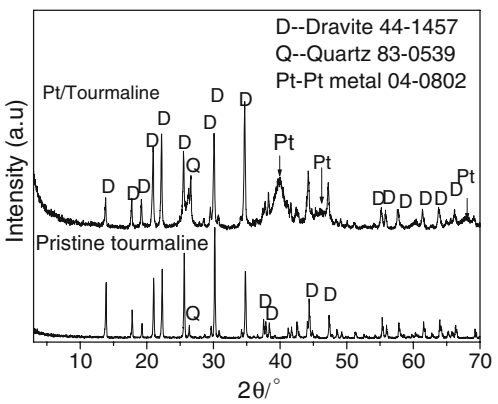

Fig. 1 XRD patterns for the catalysts of Pt/tourmaline and pristine tourmaline. *D* dravite; *Q* quartz

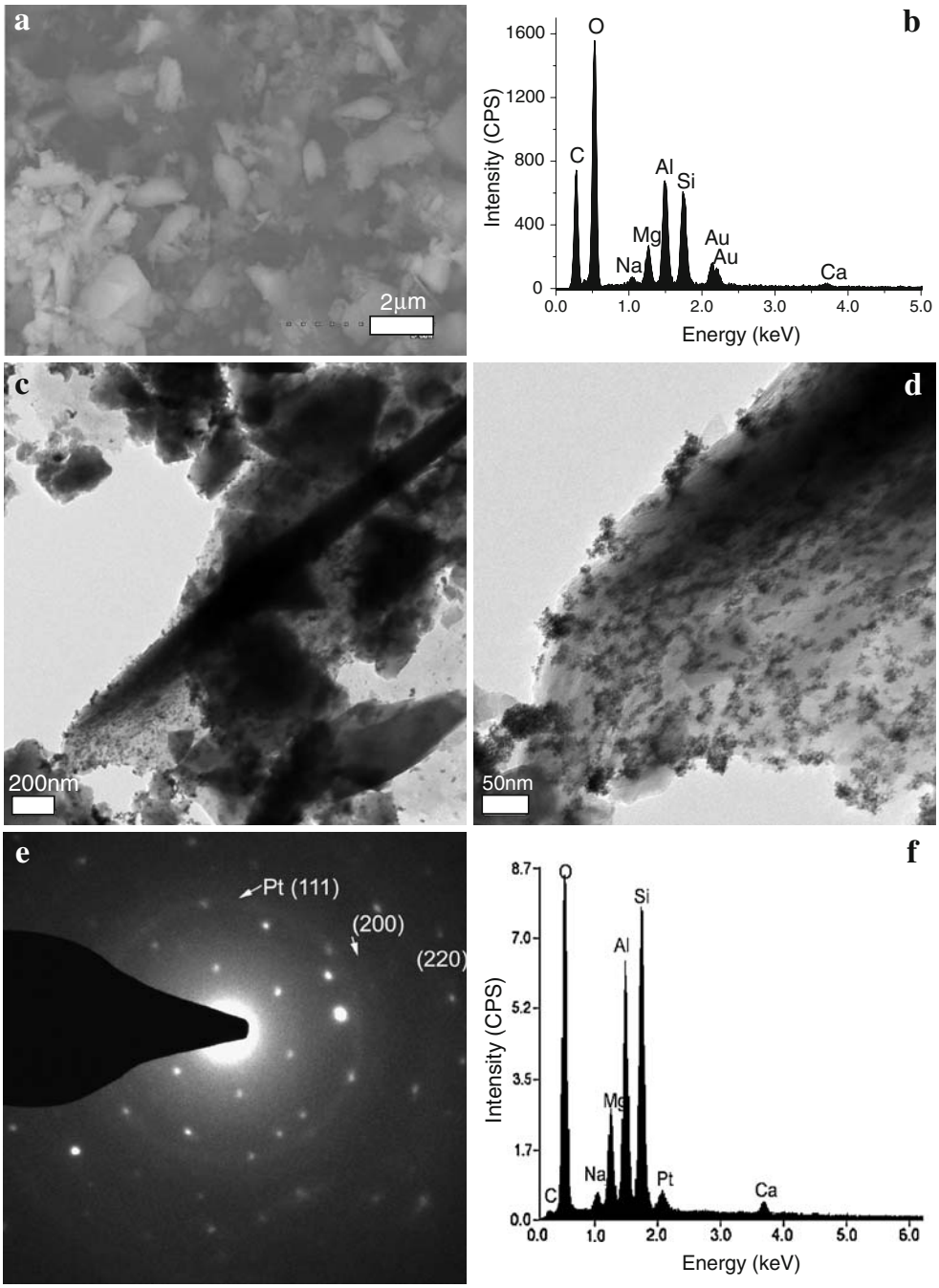

Fig. 2 **a** SEM of the pristine tourmaline; **b** EDS spectrum of the pristine tourmaline; **c**, **d** TEM images of Pt/tourmaline prepared via electrodeposition; **e** selected area electron diffraction (SAED) in area of (**c**); insert in (**c**), the data denote the diffraction rings for Pt (fcc); **f** EDS spectrum of Pt/tourmaline composite taken from the micro-area in (**c**)

ically captured using a CCD camera. Scanning electron microscopy (SEM) examination was carried out on a scanning electron microscope (JEOL JSM-6700) operated in high-vacuum mode at 15 kV linked with energy dispersive analysis system of X-ray (EDAX, Phoenix).

Electrochemical measurements were conducted on computer-controlled BAS 100 B/W electrochemical analyzer with a three-electrode cell at room temperature (~25°C), in which the prepared electrodes made in the abovementioned procedure served as the working electrode and Pt spiral wire as the counter electrode. The reference electrode was Ag/AgCl electrode. Both water–methanol and H_2SO_4 containers were de-aerated with nitrogen (99.99%) and circulated through the cell. The electrolyte solutions were prepared from H_2SO_4, methanol, and MQ water. The prepared electrodes were tested for methanol oxidation by using cyclic voltammetry (CV), from +1.0 to 0.0 V vs. Ag/AgCl, with a solution of 0.5 M methanol in 0.5 M H_2SO_4. The catalytic responses toward methanol oxidation were measured by chronoamperometry with 0.5 M methanol in 0.5 M H_2SO_4 using a constant potential of 0.51 V vs. Ag/AgCl for 450 min.

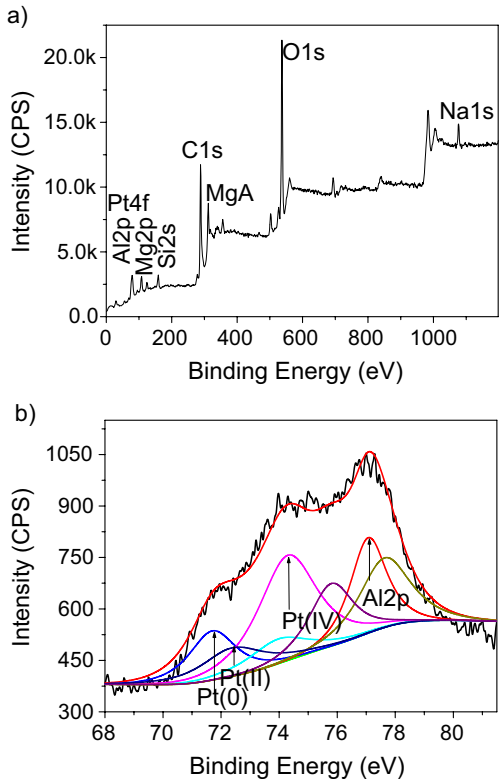

Fig. 3 XPS spectra of sample Pt/tourmaline: **a** survey spectrum and **b** high-resolution XPS Pt 4f spectrum in Pt/tourmaline

Results and discussion

Figure 1 shows the XRD patterns for the sample of pristine tourmaline and Pt/tourmaline composites. The diffraction peaks in all the diffractograms of pristine tourmaline were nearly totally indexed to dravite (JCPDS, 44-1457). The minor mineral in pristine tourmaline is mainly quartz as denoted in Fig. 1. The new peaks of Pt/tourmaline at 39.76°, 46.24°, and 67.45° were ascribed to the planes (111), (200), (220) of face-centered cubic (fcc) structure of Pt (JCPDS, 04-0802). This indicated the presence of Pt in the prepared composites. It is obvious that the peaks of Pt widen to some extent and exhibit a lower relative intensity, which indicates the small size and low degree of crystallization of the Pt nanoparticles. Based on the Scherrer equation [23], the average crystal size of the Pt particles was estimated to be about 4.5 nm by using the data for the most intensive (111) reflection.

The microstructure and morphology of the pristine tourmaline and prepared Pt/tourmaline were characterized by SEM and TEM. Figure 2a is the SEM image of the pristine tourmaline, and many column- or prism-shaped crystallites were found, which proves to be typical tourmaline crystals [20]. The EDS analysis performed during SEM observation is shown in Fig. 2b, and the result also confirmed the overweight of Mg than Fe, which suggested dravite was the main component in the pristine tourmaline, which is consistent with XRD and EPMA analysis. The detected Au element was due to spraying Au layer in the sample preparation for SEM observation. TEM morphology of Pt/tourmaline is displayed in Fig. 2c and d. It is clearly shown in Fig. 2c that numerous uniformed nanoparticles were distributed on the tourmaline crystals. And the corresponding magnified image of one tourmaline crystal is shown in Fig. 2d. The nanoparticles consisted of smaller clusters, which homogeneously assembled along the tourmaline surface. The size of the Pt single cluster is around 5 nm and this agrees well with the calculation by Scherrer equation. Selected area electron diffraction (SAED) spectrum in Fig. 2e suggests the mixture diffraction patterns for the tourmaline and the diffraction rings of Pt (fcc) [20, 24]. The EDS analysis linked with TEM also confirmed the incorporation of Pt in the composite (Fig. 2f).

The XPS analysis was used to exactly detect the covalent state of various species in the composite. Figure 3a presents the survey XPS spectrum of the Pt/tourmaline composite, and Fig. 3b shows the high-resolution XPS spectra of Pt 4f. From Fig. 3a, the mass ratio of Pt in the elements of Si, Al, Mg, Na, Ca, and O is ~0.68%, which is below the initial addition of Pt into the tourmaline. This might be due to the incomplete incorporation of Pt into the tourmaline layer by electrodeposition. The high-resolution spectrum at ca. 75.0 eV (Fig. 3b) was deconvoluted into three pairs of Pt 4f doublets and Al 2p peak (77.2 eV) that originates from the tourmaline support. The most resolved doublet is assigned to Pt(0) with peak binding energies of Pt $4f_{7/2}$ and $4f_{5/2}$ at 71.5 and 74.8 eV, respectively, which are very close to the values of Pt foil [25]. However, the other two weaker doublets suggest the presence of Pt(II) and Pt(IV), and it is suggested that there are Pt oxides likely as PtO, Pt $(OH)_2$, and $PtO(OH)_2$ in this system [26]. The existence of Pt oxide on the surface of nanometal was also reported by others, and the oxides might come from the Pt metal

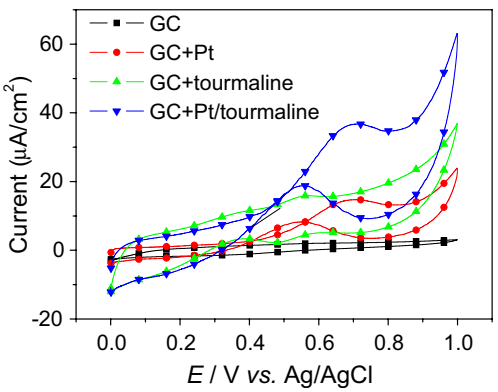

Fig. 4 Cyclic voltammograms for the electrochemical oxidation of 0.5 M methanol dissolved in 0.5 M H_2SO_4 aqueous solution and recorded at different electrodes (v=50 mV/s)

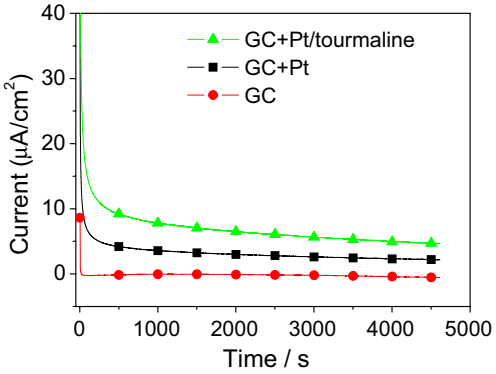

Fig. 5 Chronoamperometry of GC, Pt/GC, and Pt/tourmaline/GC in 0.5 M CH_3OH/0.5 M H_2SO_4 at 0.51 V vs. Ag/AgCl

particles when they are exposed to air for a period of time [27]. From the integral area calculated from the peaks, that metallic Pt(0) is about 34.2% of the platinum species in the composites.

Methanol oxidation reaction was carried on the GC, GC modified with Pt (Pt/GC), GC modified with tourmaline (tourmaline/GC), and the electrodeposited Pt/tourmaline/GC electrodes in 0.5 M CH_3OH and 0.5 M H_2SO_4 solutions by monitoring cyclic voltammetry. The cyclic voltammograms are shown in Fig. 4. The bare GC shows no activity in oxidation of methanol as anticipated, and Pt-modified GC anode displays oxidation peak at 0.7 V, which is ascribed to CH_3OH oxidation [28, 29]. For the tourmaline-modified GC electrode, the double peaks are observed between 0.38 and 0.60 V in the positive-going scan and between 0.30 and 0.72 V in the negative-going scan. The specific electro-reactions might be due to the redox processes of transition metals in tourmaline [30]. However, due to the permanent polarity, tourmaline particles tend to be polarized by an external electric field and are attracted to the gap between the electrodes where the field is at a maximum. It is feasible to conclude that electrostatic force would render tourmaline particles to entrap the polar molecules that exist in the proximity and thus facilitate the reaction under certain conditions [31]. As expected, a higher peak of methanol oxidation in Pt/tourmaline/GC electrode was observed at ~0.68 V and the onset potential (taken at i=9.0 μA/cm^2) was ~0.36 V vs. Ag/AgCl (Fig. 4). Compared with the onset potential (0.51 V) of the Pt/GC, a negative shift of 0.15 V was found and the current density was also increased. This indicates the enhancement of the catalytic activity of the platinum coating on GC anode with the assistance of tourmaline. Generally, the onset potential is related to the breaking of C–H bonds and subsequent removal of CO_{ad} intermediates by oxidation with OH_{ad} supplied by Pt–OH or other sources [32–34]. As known in the literature, the piezoelectricity of tourmaline gives rise to a potential difference in a constant axial direction [35], and when tourmaline was present in an applied electron field, the potential difference present within tourmaline would favor retaining electrons or charge carriers along it. The electrons and charge carriers include OH^-, O^-, O_2^-, or other negative ions [36, 37]. In the presence of this electric field, the negative ions would transform into radicals by electron transfer. Once the radicals are produced, they will surely promote the oxidation of the adsorbed intermediates to CO_2 or weaken the adsorption of CO and other intermediates, and thus a much lower potential will render the oxidation for methanol occurrence [38].

Chronoamperometry was carried out to study the time-dependent behavior of the electrodes towards methanol oxidation. Figure 5 depicts the chronoamperometry curves of GC, GC/Pt, and Pt/tourmaline/GC in 0.5 M CH_3OH and 0.5 M H_2SO_4 at 0.51 V vs. Ag/AgCl. GC shows nearly no current. Both Pt/GC and Pt/tourmaline/GC electrodes exhibit a similar current density trend. However, the current density of Pt/tourmaline/GC is higher than Pt/GC, and this might suggest the positive effect of incorporation of

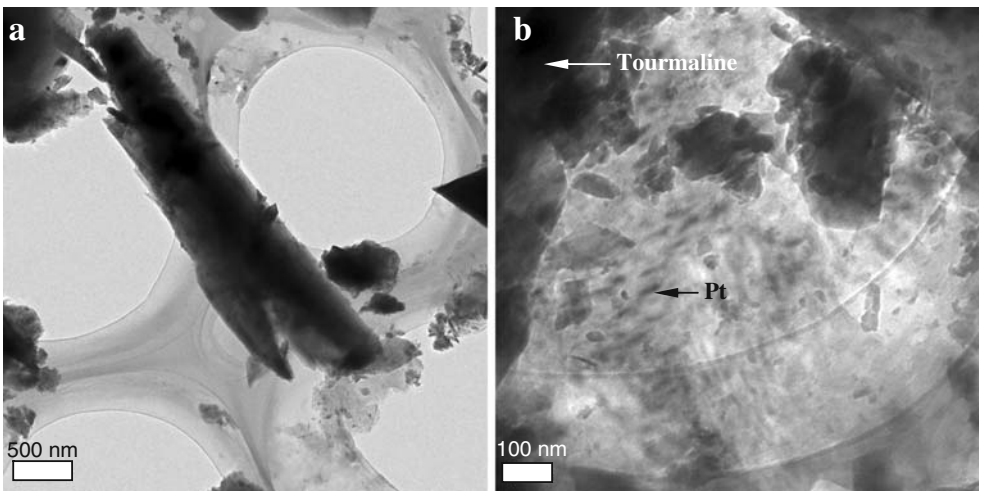

Fig. 6 TEM image of Pt/tourmaline composite from Pt/tourmaline/GC scanned in 0.5 M CH_3OH/0.5 M H_2SO_4 for ten runs

tourmaline in the composite electrode. It is noted that Pt/tourmaline/GC declined to some extent within the initial 5,000 s and the current density was still higher than that of Pt/GC, which indicates a better catalytic activity of Pt/tourmaline/GC for methanol oxidation. The current decay may be ascribed to the formation and adsorption of intermediate species such as CO, methoxy species, and other hydrocarbons on the active sites of the catalysts [1, 39–41]. Therefore, improving the stability of the Pt electrode assisted with tourmaline is the major task of the science henceforth.

To check the morphology of the used Pt/tourmaline composite, we collected the layer of Pt/tourmaline that was scanned for ten runs from GC electrode and observed under TEM. Figure 6 displayed the typical morphology in different magnification scales. From Fig. 6b, one can find some particles arranged in order in the micro-area and we indicate that Pt nanoparticles might be affected by the applied electric field and the permanent electric field from tourmaline, which altered their morphologies in the oxidation reaction. Due to the mixed electric fields, Pt can range along the surface of tourmaline after the reaction.

Conclusion

The composite layer of Pt/tourmaline was first prepared on glass carbon disk electrode via electrodeposition and the electrocatalytic activity toward the oxidation of methanol was investigated. It was indicated that the incorporation of tourmaline into the Pt/glassy carbon electrode enhanced the catalytic activity and stability towards the electro-oxidation of methanol. This method anticipates providing a new and effective approach to produce tourmaline-based electrodes or other electric devices.

Acknowledgements The project was financed by NSF of China (grant nos. 40602008, 50702006, and 50873015), NCET of China, the Beijing Municipal Science & Technology New Star Plan (2007B026), and the Research Fund of Beijing Key Laboratory of Water Resources & Environmental Engineering.

Reference

1. Aricò AS, Bruce P, Scrosati B, Tarascon J-M, Van Schalkwijk W (2005) Nature Mater 4:366
2. Wang ZB, Yin GP, Lin YG (2007) J Power Sources 170:242
3. Zhu Y, Uchida H, Yajima T, Watanabe M (2001) Langmuir 17:146
4. Maier J (2005) Nature Mater 4:805
5. Hu YS, Guo YG, Sigle W, Hore S, Balaya P, Maier J (2006) Nature Mater 5:713
6. Masanobu C, Tribidasari AI, Kamiya A, Fujishima A, Einaga Y (2008) J Electroanalytical Chem 612:201
7. Geng R, Zhao G, Liu MC, Li MF (2008) Biomater 29:2794
8. Martin HB, Argoitia A, Landau U, Anderson AB, Angus JC (1996) J Electrochem Soc 143:133
9. Shan CC, Tsai DS, Huang YS, Jian SH, Cheng CL (2007) Chem Mater 19(3):424
10. Long JW, Stroud RM, Swider-Lyons KE, Rolison DR (2000) J Phys Chem B 104:9772
11. Swain GM (1994) J Electrochem Soc 141:3382
12. Fischer AE, Swain GM (2005) J Electrochem Soc 152:369
13. Ferro S, De Battisti A (2002) Electrochim Acta 47:1641
14. Soh KL, Kang WP, Davidson JL, Wong YM, Wisitsora-at A, Swain G, Cliffel DE (2003) Sens Actuators B Chem 91:39
15. Salazar-Banda GR, Eguiluz KIB, Avarcal LA (2007) Electrochem Comm 9:59
16. Montilla F, Morallon E, Duo I, Comninellis C, Vazquez JL (2003) Electrochim Acta 48:3891
17. Tokumura M, Znad HT, Kawase Y (2006) Chem Eng Sci 61:6361
18. Xia MS, Hu CH, Zhang HM (2006) Process Biochem 41:221
19. Jiang K, Sun TH, Sun LN, Li HB (2006) J Environmental Sci 18:1221
20. London D, Ertl A, Hughes JM, GB Morgan VI, Fritz EA (2006) Am Mineral 91:680
21. Prasad PSR (2005) Gondwana Research 8:265
22. Li JH, Lu AH, Liu F, Fan LZ (2008) Solid State Ionics 179:1387
23. Eshtiagh-Hosseini H, Housaindokht MR, Chahkandi M (2007) Mater Chem Phys 106:310
24. Steigerwalt ES, Deluga GA, Lukehart CM (2002) J Phys Chem B 106:760
25. Raman RK, Shukla AK, Gayen A, Hegde MS, Priolkar KR, Sarode PR, Emura S (2006) J Power Sources 157:45
26. Zarraga-Colina J, Nix RM (2006) Surface Sci 600:3058
27. Chen L, Lu GX (2008) Electrochim Acta 53:4316
28. Frelink T, Visscher W, Cox AP, Veen JAR (1995) Electrochim Acta 40:1537
29. Park KW, Choi JH, Kwon BK, Lee SA, Sung YE, Ha HY, Hong SA, Kim H, Wieckowski A (2002) J Phys Chem B 106:1869
30. Weller MT, Dann SE (1998) Curr Opin Solid State Mater Sci 3:137
31. Zhang X, Wang JC, Lacki KM, Liapis AI (2004) J Coll Interface Sci 277:483
32. Tong Y, Kim HS, Babu PK, Waszczuk P, Wieckowski A, Oldfield E (2002) J Am Chem Soc 124:468
33. Freelink T, Visscher W, vanVeen JAR (1996) Langmuir 12:3702
34. Waszczuk P, Wieckowski A, Zelenay P, Gottesfeld S, Coutanceau C, Leger JM, Lamy C (2001) J Electroanal Chem 511:55
35. Katzir S (2003) Stud Hist Philos Sci, Stud Hist Philos Mod Phys 34:579
36. Sass AS, Shvets VA, Saveleva GA, Popova NM, Kazanskii VB (1986) Kinet Katal 27:894
37. Saveleva GA, Sass AS, Speranskaya GV, Tenchev KK, Petrov LA, Vozdvizhenskii VF, Galeev TK, Popova NM (1987) Kinet Katal 29:866
38. Campos CL, Roldán C, Aponte M, Ishikawa Y, Cabrera CR (2005) J Electroanalytical Chem 581:206
39. Watanebe M, Motoo S (1975) J Electroanal Chem 60:267
40. Munk J, Christensen PA, Hamnet A, Skou E (1996) J Electroanal Chem 401:215
41. Wang H, Wingender C, Baltruschat H, Lopez M, Reetz MT (2001) J Electroanal Chem 509:163